LANGMUIR

Article

pubs.acs.org/Langmuir

Effect of Sophorolipid *n*-Alkyl Ester Chain Length on Its Interfacial Properties at the Almond Oil–Water Interface

Amanda Koh,[†] Robert J. Linhardt,[‡] and Richard Gross*[,‡]

[†]Center for Biotechnology and Interdisciplinary Studies, Department of Chemical & Biological Engineering and [‡]Center for Biotechnology and Interdisciplinary Studies, Department of Chemistry and Biology, Rensselaer Polytechnic Institute (RPI), Biotechnology Building, 110 Eighth Street, Troy, New York 12180, United States

Supporting Information

ABSTRACT: Sophorolipids (SLs), produced by *Candida bombicola*, are of interest as potential replacements for hazardous commercial surfactants. For the first time, a series of molecularly edited SLs with ethyl (EE), *n*-hexyl (HE), and *n*-decyl (DE) esters were evaluated at an oil (almond oil)–water interface for their ability to reduce interfacial tension (IFT) and generate stable emulsions. An increase in the *n*-alkyl ester chain length from ethyl to hexyl resulted in a maximum % decrease in the IFT from 86.1 to 95.3, respectively. Furthermore, the critical aggregation concentrations (CACs) decreased from 0.035 to 0.011 and 0.006 mg/mL as the ester chain length was increased from ethyl to *n*-hexyl and *n*-decyl, respectively. In contrast, the CAC of natural SL, composed of 50/50 acidic and LSL, is 0.142 mg/mL. Dynamic IFT analysis showed significant differences in diffusion coefficients for all SLs studied. Almond oil emulsions with up to 200:1 (by weight) oil/SL-DE were stable against oil separation for up to 1 week with average droplet sizes below 5 μm. Emulsions of almond oil with natural SLs showed consistent oil separation 24 h after emulsification. A unique connection between IFT and emulsification was found as SL-DE has both the lowest CAC and the best emulsification performance of all natural and modified SLs studied herein. This connection between CAC and emulsification may be generally applicable, providing a tool for the prediction of optimal surfactants in other oil–water interfacial applications.

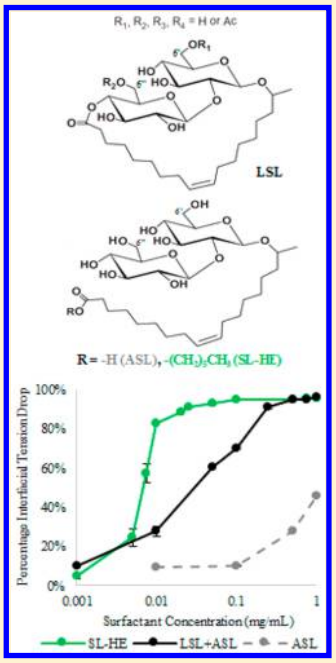

INTRODUCTION

The physical mixing of two immiscible liquid phases creates a system with high free energy at the interface. This system is thermodynamically unstable and will quickly result in the re-establishment of two bulk liquid phases. However, there is great interest in mixing hydrophobic and hydrophilic components, such as water and hydrophobic antibiotics or flavor/scent oils, to form emulsions with excellent stability. The introduction of an amphiphilic surfactant, which adsorbs preferentially to the liquid/liquid interface, allows for the reduction of the system's free energy and the stabilization of some interfacial area. These liquid/liquid dispersions are typically called emulsions.

The overall reduction in free energy is measured as a reduction in surface or interfacial tension, and the stability of the resulting emulsion when using a particular surfactant has been studied for decades. Surfactant emulsion performance is dependent on many factors, including homogenization, the relative composition and concentration of the hydrophilic and hydrophobic phases, and the surfactant structure.[1] Although the hydrophilic and hydrophobic phases are generally dictated by the application and homogenization is confined by what is easily scalable, the surfactant structure can be fine-tuned to alter the emulsion performance.

Although a broad range in synthetic surfactants has been studied over the past century, there is increasing public concern over their production from nonsustainable feedstocks, toxic chemical intermediates (e.g., ethylene oxide), and toxic byproducts.[2,3] Consequently, there is increased interest in the development of natural surfactants produced by microbes because they result from fermentation processes that convert readily renewable feedstocks such as glucose and triglycerides under mild conditions to safe fully biodegradable products.[4,5] Their use in industrial applications requires that we better understand the performance of natural biosurfactants as well as modified forms prepared by simple and scalable chemical methods.

Sophorolipids (SLs) are biosurfactants of glycolipids produced in large quantities by fermentation of yeasts such as

Received: March 14, 2016
Revised: May 2, 2016
Published: May 9, 2016

 © 2016 American Chemical Society DOI: 10.1021/acs.langmuir.6b01008

Candida bombicola.[6−8] As shown in Scheme 1, natural sophorolipids consist of sophorose (2-*O*-*β*-D-glucopyranosyl-

Scheme 1. Structures of Lactonic and Acidic Sophorolipids,Which Are the Natural Products Formed by the Fermentation of *Candida bombicola* on High Oleic Acid Carbon Sources[a]

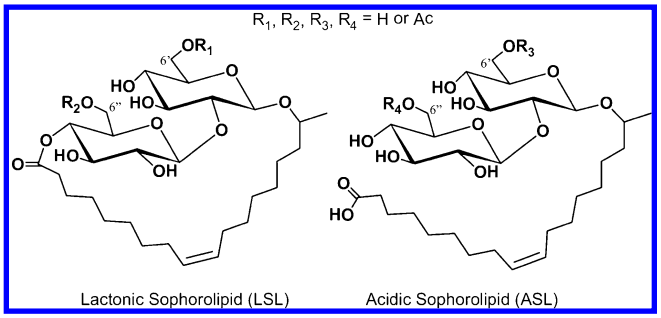

[a]6′ and 6″ carbons are highlighted as the positions of potential acetylation.[26]

α-D-glucose or *β*-D-Glc-(1 → 2)-D-Glc) bound to a hydroxy fatty acid (e.g., 17-hydroxy-9-*cis*-octadecenoic acid, 17-HOC18:1Δ^9) through a glycosidic linkage. It is well known in the literature that when using high oleic acid as a feedstock, in addition to the most abundant hydroxyl fatty acid (17-HOC18:1Δ^9), sophorolipids also contain other chain length fatty acids (e.g., 16-hydroxyfatty acid) and hydroxylation at the terminal position.[9] The sophorose moiety may contain acetyl groups at the 6′ and/or 6″ positions, and the molecule is formed as a mixture of its lactonic (LSL) and ring-opened (e.g., acidic, ASL) forms.

SLs have attracted considerable commercial attention because of the availability of safe strains that produce them in high yields (>400 g/L) and the development of applications where they are useful.[7] SLs are being produced/developed commercially by Ecover, France-based Soliance/WheatOleo, Japan-based Saraya, South Korea-based MG Intobio, U.S.-based SyntheZyme, and Japan-based Allied Carbon Solutions (ACS) for applications in cosmetics, detergents, and more.[10]

The critical micelle interfacial properties of natural SLs have been previously evaluated for SLs produced by various strains. Critical micelle concentrations (CMCs) ranging from 20 to 130 mg/L and minimum surface tensions (mSFTs) from 32 to 42 mN/m were reported.[11−14] The initial foaming capability of LSL has been studied by Hirata et al.[12] Daverey et al.[13] and Ma et al.[14] described the emulsification activity of LSL after 24 h and 10 m, respectively, using 50 vol % of the hydrophobic phase. Maddikeri et al.[15] and Daverey et al.[13] published interfacial tension (IFT) measurements with LSL at one surfactant concentration (500 and 200 mg/L, respectively) with various oils. For other surfactants such as plant and milk proteins and sorbitan monooleate (Span 80), relationships among emulsion stabilization, interfacial elasticity,[16] interfacial and bulk viscosity,[17,18] and IFT[19] were addressed. Furthermore, the critical aggregation concentration (CAC) has rarely been reported in the surfactant literature. Moreover, relationships among the CAC, max % IFT, and emulsification performance have thus far been overlooked. Also, the influence of LSL's low water solubility on the natural SL emulsion stabilization has largely been neglected.

Studies have been performed to modify the SL structure during microbial production to enhance or modulate SL performance in applications. Strategies thus far employed include varying media components including the fatty acid carbon source[20,21] and genetic engineering of the production strain to alter the biosynthetic pathway.[22,23] These approaches have resulted in substantially reduced product yields and/or severe SL mixtures (e.g., varying hydroxyfatty acid lengths and degree of unsaturation). Furthermore, both genetic engineering and feedstock variation have substantial limitations with respect to the extent of structural variation that can be achieved.

Our laboratory has developed a suite of simple and scalable methods for natural SL postmodification to gain a comprehensive understanding of SL structure−property relationships. The preparation of SL ester derivatives by LSL ring opening, under alkaline conditions using selected alcohols as the reactant and solvent, is one example that is used herein.[24] Further variation of SL-ester structure has been achieved by enzyme-catalyzed selective acylation at the two sophorose primary hydroxyl moieties at C6′ and C6″ (Scheme 1).[25] Other examples include the conjugation of amino acids to the SL fatty acid carboxylic acid moiety[25] and the ring-opening cross metathesis (RO/CM) of LSLs using a variety of olefin substrates.[26] Hence, chemical transformations of SLs allow access to a large library of modified SL structures that enable in-depth studies of modified SL structure−property relationships. In this article, LSL ring opening under alkaline conditions with

Scheme 2. Structures of SL-EE, SL-HE, and SL-DE

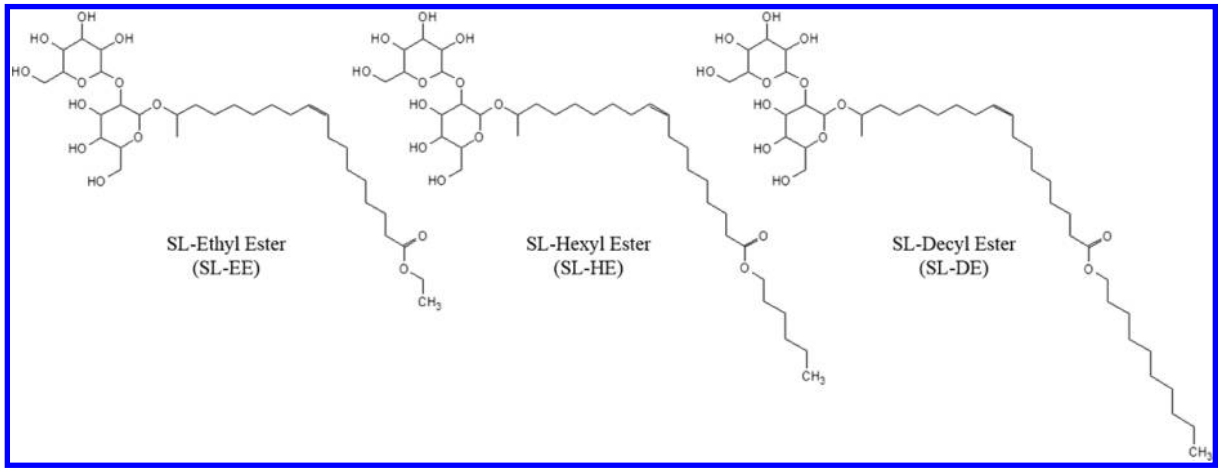

DOI: 10.1021/acs.langmuir.6b01009

ethanol, hexanol, and decanol was performed to prepare SL-ethyl ester (SL-EE), SL-hexyl ester (SL-HE), and SL-decyl ester (SL-DE), respectively (Scheme 2). By this approach, the hydrophobic moiety of SLs is extended from 18 (17-HOC18:1Δ^9) to 20, 24, and 28 carbons, respectively.

Only a few journal publications describe the interfacial properties of modified SLs. Zhang et al.[27] published values of mSFT and CMC for a series of *n*-alkyl SL-esters where the *n*-alkyl moiety was varied from methyl to hexyl. Shin et al.[28] reported foaming, CMC, and mSFT values for SL-methyl ester. However, previous work has not addressed the effects of SL modification on oil/water interfacial properties. Hence, a series of SL-esters (SL-EE, SL-HE, and SL-DE) were synthesized and studied herein to determine how the extension of the primary hydrophobic unit, 17-HOC18:1Δ^9, by relatively small *n*-alkyl groups after interruption by an ester moiety influences interfacial activity and emulsification. This work focuses on three sophorolipid derivatives: SL-EE, SL-HE, and SL-DE as shown in Scheme 2.

Almond oil was selected as the oil phase for the studies performed. The world production of almonds in 2011 reached 2.00 million tons, and the United States is the largest producer at 0.73 million tons.[29] Almond oil primarily consists of triglycerides in which oleic and linoleic acids comprise about 70 and 20%, respectively, of triglyceride fatty acids.[30] Almond oil is widely used in food and personal care products. Its function in the latter is as an emollient for moisturizers, hair products, and antiaging creams.[31−33] It is hypothesized that, from studies of this important triglyceride plant oil, fundamental information will result that provides important insights that can be applied to the design of modified SLs for this and other triglyceride-based oils such as olive, palm, and corn oils.

This article reports on IFT reduction at the almond oil/water interface as a function of SL-ester structure and concentration. To provide a quantitative method for this analysis, plots of IFT reduction vs SL-ester concentration were generated. These plots were used to determine what we define herein as the critical aggregation concentration (CAC). From IFT measurements, we report corresponding values of diffusion coefficients, maximum IFT reduction (max % IFT), and CAC for each oil/surfactant pair. Emulsions of almond oil, water, and SL-esters, with varying oil and SL-ester concentrations, were analyzed over time to determine if phase separation and changes in average droplet size occur. For comparison to natural SLs produced as mixtures, IFT reduction and emulsification properties were also evaluated using a 1:1 w/w LSL + ASL mixture.

EXPERIMENTAL SECTION

Materials. Almond oil from the *Prunus dulcis* tree was purchased from Sigma-Aldrich and used as received. For all of the studies performed herein, the almond oil used is from the same batch, which was stored at 4 °C in an amber glass container to minimize variation and degradation. All water used for these experiments was Millipore deionized water.

Sophorolipid (SL) Production via Fermentation. SLs were synthesized by the fermentation of *Candida bombicola* as previously reported from high oleic acid content sunflower oil.[26] Further information on the fermentation process and product isolation is given in the Supporting Information. The resulting solid was a mixture of LSL and ASL with varying degrees of acetylation as shown in Scheme 1. However, the major product, based on analysis by liquid chromatography−mass spectrometry (LC−MS) following a literature method,[34] contained about 95 mol % diacetylated lactonic sophorolipid.[9] NMR and LC−MS analysis of ASL[25] and LSL[34] have been previously published.

Synthesis of SL-Esters. A literature procedure was followed to prepare SL-EE and SL-HE, and a modification of this method was used to prepare SL-DE.[24] Details of the synthesis method used are given in the Supporting Information.

Interfacial Tension. Interfacial tension (IFT) measurements of SL-EE, SL-HE, SL-DE, and 1:1 w/w LSL + ASL were performed using a Krüss DSA100 drop shape analyzer (Hamburg, Germany) at concentrations from 0.001 to 1 mg/mL. In addition, ASL IFT reduction was measured up to 50 mg/mL. IFT was analyzed at each concentration, and measurements were recorded after equilibrium was reached. Diffusion coefficients were calculated by the short-time approximation (limit of $t \rightarrow 0$) (eq 2) of Ward and Tordai's diffusion-controlled adsorption relationship shown in eq 1:

$$M = 2\sqrt{\frac{D}{\pi}} \int_0^{\sqrt{t}} \varphi(t) d\sqrt{t-\tau} \tag{1}$$

$$\frac{\gamma(t) - \gamma_0}{\sqrt{t}} = -2RTC\sqrt{\frac{D_{ap}}{\pi}} \tag{2}$$

In eq 1, M is the surfactant concentration, D is the diffusion coefficient, φ is the surface surfactant concentration, and τ is a dummy integration variable. In eq 2, $\gamma(t)$ is the interfacial tension at time t, γ_0 is the pure oil/water interfacial tension (26.5 mN/m for the almond oil used), C is the bulk surfactant concentration, and D_{ap} is the apparent diffusion coefficient.[35,36] For each time, the sample chamber was cleaned, a new volume of almond oil was used, and the pure water IFT was measured to ensure oil integrity.

Equilibrium IFT measurements were used to calculate minimum IFT values for each SL-ester. Minimum IFT values are the average of at least three consecutive IFT measurements in the concentration-independent range where IFT no longer decreases. IFT reduction values at each concentration are reported as the percent (%) IFT decrease and were calculated by eq 3

$$\%\text{IFT decrease} = \frac{\gamma_0 - \gamma}{\gamma_0} \times 100 \tag{3}$$

where γ_0 is the pure oil/water interfacial tension and γ is the equilibrium interfacial tension for that concentration. CAC values are reported in mg/mL and mol/L. Each is the x value at the intersection of a line drawn through at least three points in the concentration-dependent region and through at least three points in the concentration-independent region.

Emulsification. Emulsions of almond oil were formed in deionized water using an IKA T25 shear homogenizer with mixing at 24 000 rpm for 60 s. Oil concentrations of 1, 10, and 20 wt % and SL-ester concentrations of 0.1 and 1.0 wt % were evaluated. All weight percentages are based on the total emulsion weight. Emulsions were analyzed immediately and/or after aging at 25 °C in a temperature-controlled incubator for 24 h and 1 week.

Droplet size measurements were determined with a Malvern Zetasizer ZSP (Worcestershire, U.K.) using a 173° backscattering angle. All emulsions were diluted 100-fold with deionized water to avoid multiple scattering effects. Droplet sizes are reported as the mean droplet diameter (z average) in nanometers. Emulsion phase stability was recorded with photographs at each analyzed time point with a Nikon D5200 camera fitted with a Nikon AF-S Micro Nikkor 60 mm lens.

RESULTS AND DISCUSSION

Effect of SL-Ester Concentration on IFT. As amphiphilic molecules, surfactants orient preferentially such that the lipophilic region of the surfactant interacts with the lipophilic phase and the hydrophilic region interacts with the hydrophilic phase, thus decreasing the IFT. By doing so, the surfactant

DOI: 10.1021/acs.langmuir.6b01090

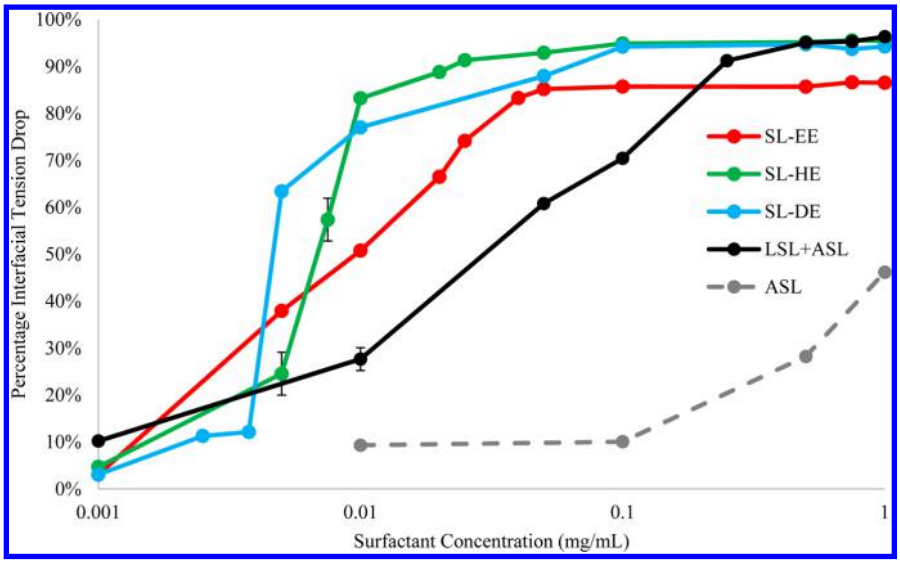

Figure 1. Percentage interfacial tension decrease across surfactant concentrations for SL-EE, SL-HE, SL-DE, LSL+ASL, and ASL measured at room temperature. Mean and standard deviation values are measured from at least three replicates.

decreases the free energy between the two immiscible phases characterized by

$$\Delta G = \gamma \Delta A \tag{4}$$

where γ is the IFT of the system and ΔA is the interfacial area.[37]

As in surface tension measurements, IFT is a function of the surfactant concentration. As the surfactant concentration increases and more molecules adsorb to the interface, a gradual reduction of the oil/water IFT occurs. At a concentration designated herein as the CAC, there is no net increase in surfactant concentration at the interface and micellar aggregates begin forming in the bulk water solution. Above the CAC, a minimum IFT is reached such that further addition of surfactant to the system will result in no additional IFT reduction but instead more micellar aggregates.[38] This behavior is identical to what occurs when measuring the CMC at the air−water interface; consequently, the analysis of CAC parallels that of CMC. The term CAC is used here instead of CMC to denote that measurements are conducted at an interface of two liquids rather than at a "surface" of air and water.

Scheme 2 shows the structures of SL-esters that were synthesized from a natural mixture containing 95% LSL. The conversion of LSL to SL-esters was accomplished by a literature method in which LSL is dissolved in an excess of the alcohol that corresponds to the *n*-alkyl ester to be synthesized. LSL ring-opening transesterification reactions were conducted at 80 °C for 3 h with a sufficient quantity of the corresponding alcohol sodium salt. As a result of the reaction conditions, the product formed is nonacetylated. Furthermore, prior to studies with SL-esters they were purified by column chromatography to remove residual fatty acids and other potential impurities. ^{1}H and ^{13}C NMR spectra of SL-esters shown in the Supporting Information are consistent with those expected.

Figure 1 displays the percent IFT drop at the almond oil/water interface for SL concentrations from 0.001 to 1 mg/mL. Except for ASL, studies at higher SL concentrations were restricted by compound solubility. SL-HE and SL-DE show similar % IFT reduction vs concentration plots. In contrast, IFT decreases relatively slower with increasing SL-EE concentration and plateaus at a lower % IFT reduction. Values of the maximum IFT tension decrease (max % IFT), and the CACs for each SL-ester are compiled in Table 1. Max % IFT values

Table 1. Critical Aggregation Concentrations (CACs) and Max % Interfacial Tension Decreases (Max % IFT Drop) for SL-EE, SL-HE, SL-DE, LSL + ASL, and ASL[a]

	critical aggregation concentration		
	(mg/mL)	(mol/L)	max % IFT drop
SL-ethyl ester	0.035	5.34×10^{-5}	86.1 ± 0.5
SL-hexyl ester	0.011	1.54×10^{-5}	**95.3 ± 0.2**
SL-decyl ester	**0.006**	**7.56×10^{-6}**	94.2 ± 0.2
LSL + ASL	0.142		**95.6 ± 0.6**
ASL	>50	>0.08	n.d.

[a]Reported values are from an analysis of the almond oil/water percent interfacial tension reduction vs surfactant concentration plots. [b]n.d. denotes not determined. Mean and standard deviations are measured from at least three replicates.

for SL-HE and SL-DE are similar (about 95%), whereas, the max % IFT for SL-EE is 86.1%. Furthermore, both molar and weight CAC concentrations increased in the following order: SL-DE < SL-HE < SL-EE (Table 1). The CAC of SL-DE was almost 6 times lower than that of SL-EE. In other words, a concentration about 6 times higher of SL-EE relative to that of SL-DE is required to saturate the almond oil−water interface. At concentrations of SL-esters where the almond oil−water interface is saturated with these compounds, SL-EE is the least effective SL-ester at reducing the IFT.

The minimum IFT values of 1.2 and 1.5 mN/m for SL-HE and SL-DE, respectively, are lower than those reported for soybean oil with polyglycerol polyricinoleate (PGPR, 6.7 mN/m) and sorbitan monooleate (Span 80, 2.9 mN/m), and the minimum IFT of lecithin (1.2 mN/m) is similar to those of SL-HE and SL-DE.[19] Because PGPR is a polymeric surfactant and lecithin is anionic, their structures differ significantly from those of neutral, low-molar-mass SL-esters. Furthermore, for emulsion preparation, PGPR, Span 80, and lecithin are all first dissolved in the oil phase. In contrast, emulsions of SL-esters are prepared by first dissolving them in the water phase and, thereafter, mixing the oil and water phases. This difference

DOI: 10.1021/acs.langmuir.6b01009

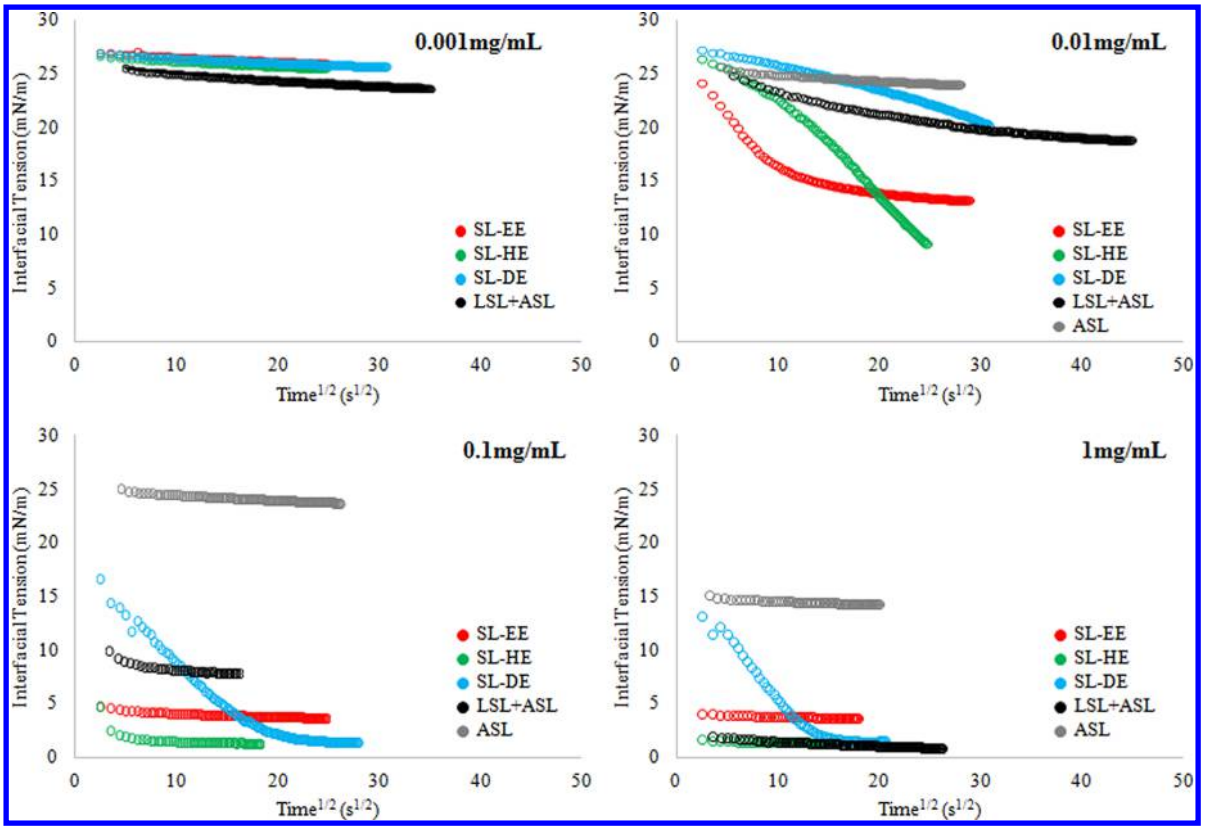

Figure 2. Dynamic IFT plotted as a function of $t^{1/2}$ at room temperature for SL-esters, LSL + ASL 1:1 w/w, and ASL concentrations ranging from 0.001 to 1.0 mg/mL.

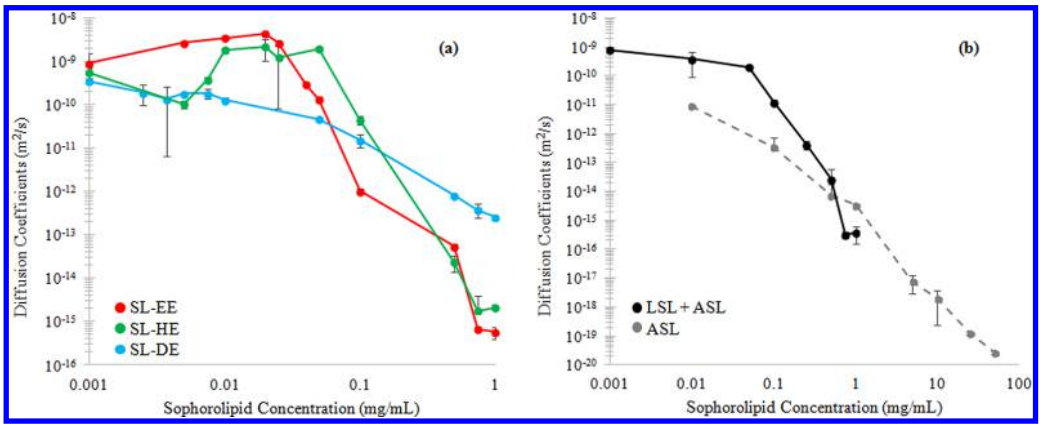

Figure 3. SL-ester diffusion coefficients (a) and natural SL diffusion coefficients (b) measured at room temperature. Note that the *x* axes for these two plots are scaled differently. Mean and standard deviation values are measured from at least three replicates.

in methodology may also impact the relative interfacial diffusion and adsorption values reported.

Figure 1 also shows the % IFT reduction for ASL and LSL + ASL (1:1 w/w). The % IFT decrease for LSL + ASL increases more slowly than for all three SL-esters but plateaus at a similar value to SL-HE and SL-DE. An analysis of the plot in Figure 1 resulted in a CAC for LSL + ASL of 0.142 mg/mL, which is 4 times higher than for SL-EE that has the highest CAC of the SL-esters studied herein. The max % IFT reduction of LSL + ASL is equivalent to SL-HE, the SL-ester with the largest IFT reduction. This is slightly higher than the minimum IFT values (3.44 and 4.46 mN/m) of an LSL + ASL natural mixture with sunflower oil and olive oil, respectively.[13] The percent IFT reduction was measured for ASL for up to 50 mg/mL, and values of up to 1 mg/mL are shown in Figure 1. The % IFT decrease with increasing ASL concentrations rises much more slowly that the LSL + ASL mixture such that the max % IFT reduction value was not reached until 50 mg/mL. The LSL % IFT reduction was not measured because of its low solubility in water (<0.1 mg/mL).

Effect of Structure on Dynamic IFT. Measurements of IFT vs time (t) were performed to better understand SL-ester interactions at the almond oil−water interface. Plots of IFT vs $t^{1/2}$ are displayed in Figure 2 for SL concentrations of 0.001, 0.01, 0.1, and 1 mg/mL. From Figure 2, it is evident that the dynamic interfacial properties of the SL-esters are inextricably linked to the SL-ester *n*-alkyl chain length and concentration. To further explore these structure−interfacial property

DOI: 10.1021/acs.langmuir.6b01009

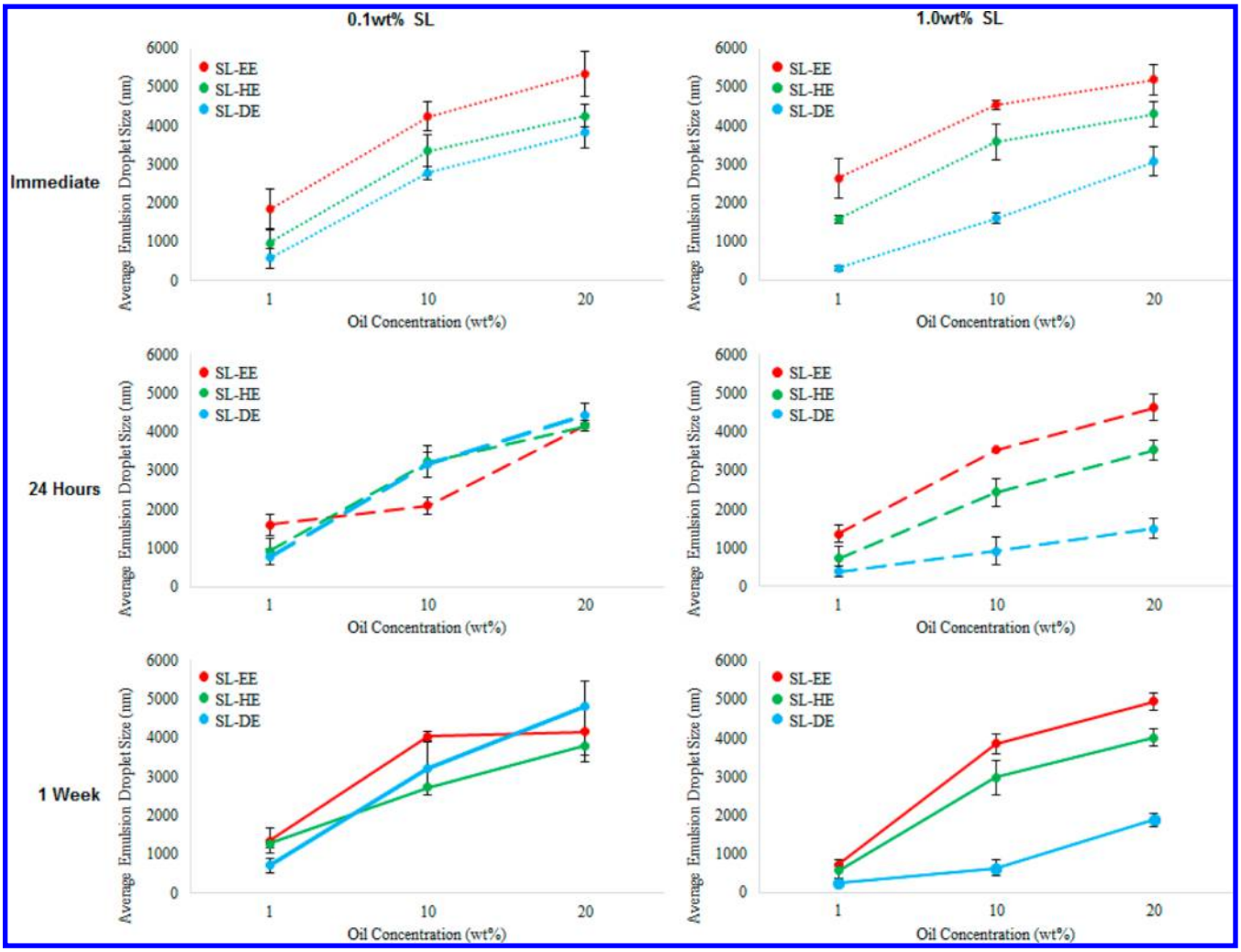

Figure 4. Average emulsion droplet sizes for SL-EE, SL-HE, and SL-DE immediately after homogenization as well as after 24 h and 1 week of aging at 25 °C. Mean and standard deviation values are measured from at least three replicates.

correlations, diffusion coefficients were calculated using data from the initial linear portion of plots of IFT vs $t^{1/2}$. The slope of the linear region was calculated from a linear regression fit of at least three data points with $R^2 > 0.9$.

Figure 3a shows the diffusion coefficients of SL-EE, SL-HE, and SL-DE as a function of SL-ester concentration. The behavior of each SL-ester is slightly different, but all three show a peak in the diffusion coefficient at their respective CAC and a significant decrease in the diffusion coefficient thereafter. Below 0.01 mg/mL, SL-EE has the highest diffusion coefficient, which is attributed to its shorter *n*-alkyl ester chain length. The diffusion coefficient of SL-EE then decreases at concentrations higher than its CAC (0.035 mg/mL). The SL-HE diffusion coefficient increases as its concentration approaches the CAC (0.011 mg/mL); thereafter, the diffusion coefficient remains constant until 0.05 mg/mL and then steadily decreases at higher SL-HE concentrations. The plot of the SL-DE diffusion coefficients shows a change in slope around its CAC (0.006 mg/mL); thereafter, it decreases at higher concentrations but at a slower rate than for SL-EE and SL-HE.

The trend that the diffusion coefficients of SL-esters decrease at concentrations above their CAC is attributed to crowding at the interface. At bulk concentrations higher than the CAC, the oil/water interface is saturated and movement onto the interface is restricted. As the bulk SL concentration increases, intermolecular repulsion from sugar headgroups will increase, further restricting SL movement at the oil−water interface, resulting in decreases in the diffusion coefficient.

At the highest concentrations examined, SL-EE and SL-HE exhibit similar diffusion coefficients whereas SL-DE has a diffusion coefficient that is 3 orders of magnitude larger. However, from Figure 2 at 0.1 and 1 mg/mL, SL-DE takes the longest time to reach equilibrium of the three SL-esters. This suggests that interfacial tension reduction resulting from SL-DE is overall kinetically controlled rather than diffusion controlled. Kinetically controlled behavior may be indicative of a different oil−surfactant interaction for SL-DE as compared to that of SL-EE or SL-HE.

Plots of diffusion coefficients of LSL + ASL (1:1 w/w) and pure ASL are shown in Figure 3b. The diffusion coefficients of ASL consistently decrease as its concentration increases, with no peak or plateau confirming that the CAC has not been reached within the range of concentrations measured. Furthermore, diffusion coefficients of ASL are consistently lower than those of the SL-esters. The LSL + ASL plot shows a change in slope after a concentration slightly higher than the calculated CAC, which may be due to the more surface active contribution of LSL. The overall curve of LSL + ASL is similar

DOI: 10.1021/acs.langmuir.6b01000

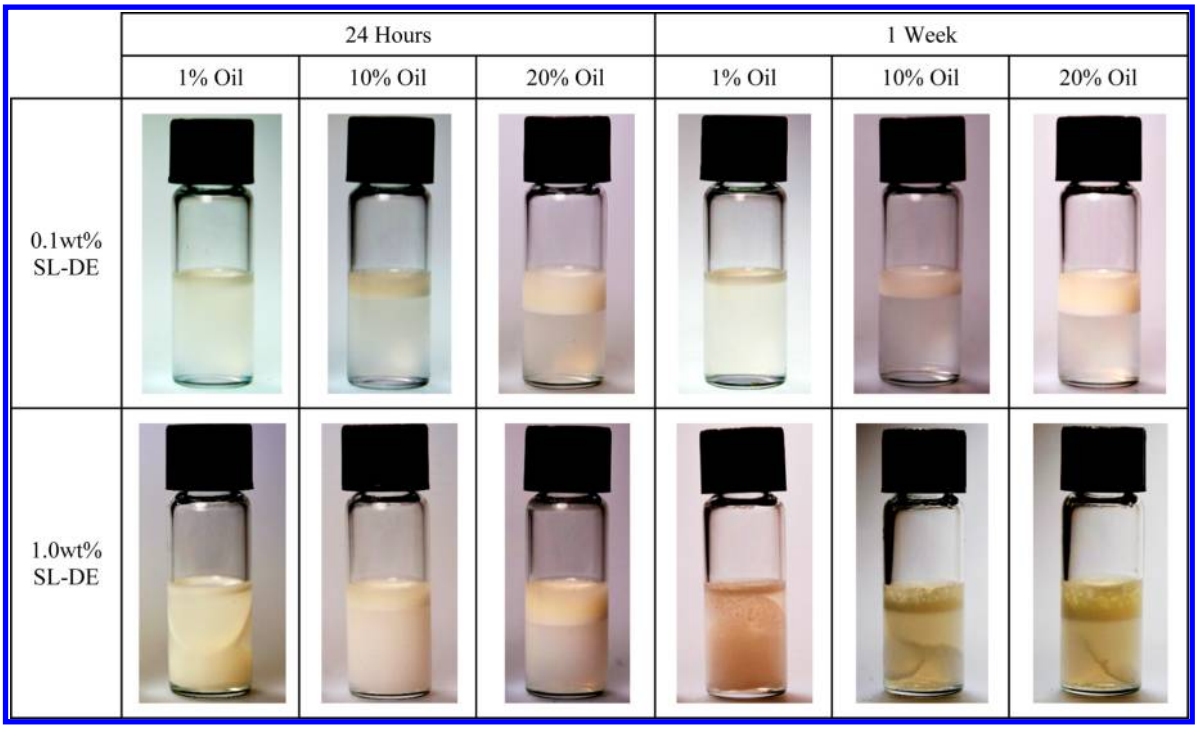

Figure 5. SL-DE emulsion physical appearance as a function of SL-DE and almond oil concentrations after 24 h and 1 week of aging.

to that of SL-EE and SL-HE in magnitude and shape, suggesting that the reduction in almond oil/water interfacial tension is influenced more by kinetic than by diffusive interactions.

Effect of Sophorolipid Structure and Concentration on Emulsion Droplet Size. As discussed above, an important characteristic of surfactants is their ability to adsorb to immiscible phase interfaces and decrease the interfacial tension. Equation 4 shows that decreasing the interfacial tension allows for increases in the interfacial area with decreased system free energy. In other words, emulsification creates a new interfacial area that requires a surfactant for stabilization. Emulsions are inherently thermodynamically unstable because energy must be added to break up the dispersed phase into droplets.[37] However, an efficient surfactant can increase the dispersed phase stability. The goal is to increase the dispersed phase stability for a sufficient time to meet the needs of a particular application prior to inevitable phase separation caused by emulsion thermodynamic instability. In other words, the ability of a surfactant to stabilize a dispersed phase is the yardstick against which surfactant application performance is often measured. On a short time scale, this is investigated through droplet size measurements and overall phase stability. The smaller dispersed emulsion droplets are more kinetically stable and, consequently, more effective at combating thermodynamic instability.[39] Furthermore, phase stability is important to investigate both as a measure of applicability to a final product and as a measure of overall emulsion stability. Microscopic phase instability denotes the bulk separation of oil from the aqueous phase or precipitation of the surfactant from the emulsion. Macroscopic phase instability describes an emulsion system that remains dispersed but is nonhomogenous throughout (i.e., creaming, flocculation, etc.).

Figure 4 shows the mean droplet size of almond oil emulsions with SL-EE, SL-HE, and SL-DE at 0.1 and 1 wt % and with almond oil concentrations of 1, 10, and 20 wt %. Each plot displays the mean droplet size immediately after emulsification and for aging times of 24 h and 1 week. Mean droplet sizes for all SL-ester/almond oil emulsions are at least 10 times smaller than those reported in the literature for soybean oil/Span 80 and lecithin soybean emulsions (droplet sizes of 59.55 and 73.37 μm, respectively) that (i) were prepared using 5 times the homogenization energy as that employed herein, (ii) contained an unspecified surfactant concentration, and (iii) used twice the amount of the oil phase (40%) studied herein.[19] Another study evaluated the emulsification of a vegetable oil with polysorbate surfactants using a water/surfactant/oil ratio of 0.8:0.1:0.1 and a similar homogenization method. Even at this high surfactant concentration, the mean droplet sizes are generally >10 μm.[40] Consequently, SL-esters have improved emulsification performance when compared to many currently used commercial surfactants.

At 0.1 wt %, little difference is seen in the droplet size across the time points. Average emulsion size as a function of the oil concentration for each SL-ester at one aging time is shown in Supporting Information. This reveals that, even at 0.1 wt % SL-ester, the SL-esters provide high emulsion stability for emulsions with almond oil concentrations 200 times (w/w) that of the surfactant. Similarly, at 1 wt % SL-ester, there is little change in the average droplet sizes from 24 h to 1 week after emulsification, revealing high emulsion stability. However, for the SL-esters at 1 wt %, the average droplet sizes immediately after emulsion formation are higher than at 24 h and 1 week. This is attributed to significant foam formation at this surfactant concentration. Dynamic light scattering does not distinguish between air bubbles and emulsion droplets, which will skew the average droplet size to higher values. The increased formation of foam for emulsions with higher surfactant concentrations is consistent with other work.[41] However, these air bubbles are not sufficiently stable to contribute to the average emulsion droplet sizes at 24 h or 1 week. The lack of air bubbles for

DOI: 10.1021/acs.langmuir.6b01909

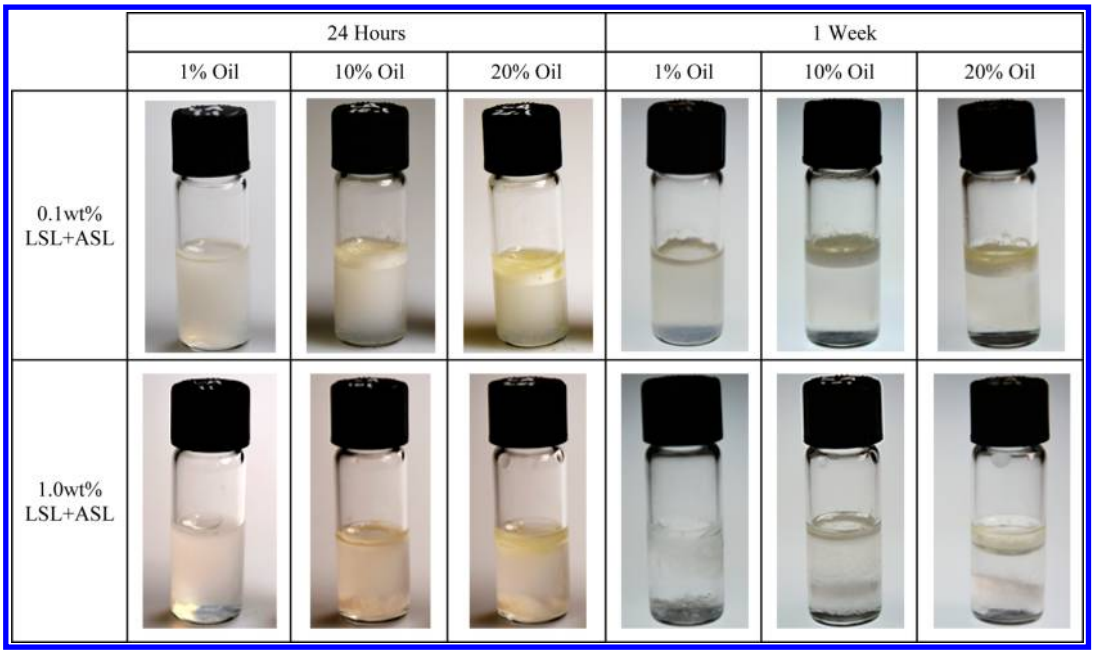

Figure 6. Physical appearance of LSL + ASL 1:1 w/w emulsions of almond oil as a function of surfactant and oil concentrations after 24 h and 1 week of aging.

emulsions aged for 24 h and 1 week was confirmed with optical microscopy. Also, because larger oil concentrations subjected to the same mixing conditions (Experimental Section) will expose less oil surface area for fixed surfactant concentrations, it follows as is observed herein that the average emulsion droplet size increases with increasing oil concentration.

At 0.1 wt % SL-ester, differences in droplet size between the different SL-ester structures are small. However, at 1 wt % SL-ester, significant differences in the average emulsion droplet sizes are seen as a function of the SL-ester structure (Figure 4). Generally, the relationship between emulsion size and SL-structure at 1 wt % is as follows: SL-EE > SL-HE > SL-DE. Hence, of the three SL-esters studied herein, SL-EE is least capable of stabilizing an almond oil emulsion whereas SL-DE has the highest emulsification activity. This trend is consistent with the relative order of CAC values as a function of surfactant *n*-alkyl ester chain length (Table 1). This may be counter-intuitive, as from eq 4 one might predict that the emulsion size trend would conform to the relative order of max % IFT decrease, particularly as all of the emulsions are formed at SL-ester concentrations orders of magnitude above the CAC's. However, IFT measurements are performed at equilibrium, when surfactants have had sufficient time to orient properly to reach their maximum IFT reduction. Furthermore, the CAC is the concentration at which the surfactant has saturated the oil/water interface and begun to form micelles. The concentration at which saturation occurs during emulsification must be significantly higher as more interfacial area is present. Nevertheless, the interfacial area of almond oil available for CAC measurements is kept constant for all SL-esters. Similarly, because homogenization is performed under identical conditions, the total interfacial area created during emulsification studies is also constant for emulsification studies with the different SL-esters. The role of the surfactant is to stabilize that interfacial area; the SL-ester structure with the lowest CAC requires the lowest concentration to perform that task. Similarly, the SL-ester during emulsification experiments that can stabilize the highest surface area will result in the smallest average oil droplet size. This explains why SL-DE, the SL-ester structure with the lowest CAC, forms emulsions with the smallest average oil droplet size.

Effect of Sophorolipid Structure on Emulsion Phase Stability. Average emulsion droplet size is not the only indicator of emulsion stability. As mentioned above, phase stability is also important to assess how a surfactant will perform as an emulsifier. The optimal emulsion is homogeneous with no bulk separation of oil or surfactant. The opacity of the emulsion can give an indication of the droplet size in different regions of the emulsion.

Figure 5 shows the physical appearance of SL-DE emulsions after 24 h and 1 week for all six formulations tested. Images of emulsions immediately after they were made are not shown because the large amount of foam obscured the separation of phases. All 1 wt % SL emulsions showed significant precipitation, but 0.1 wt % emulsions generally showed little or no precipitation across the aging times. Although none of the SL-DE/almond oil emulsions have oil separation, they all show creaming. Photographs of SL-HE and SL-EE across time and formulations showed a similar physical appearance to SL-DE.

All SL-ester emulsions undergo significant creaming, which is expected as a result of the above micrometer sizes of most emulsions. Because SL-esters are neutral, there is no electrostatic repulsion between headgroups, which may lead to a more physically homogeneous sample.[42] Nevertheless, none of the SL-ester emulsions studied herein showed a bulk separation of almond oil, even after 1 week for emulsion compositions consisting of oil concentrations 200 times that of surfactant by weight.

For emulsions with 1 wt % SL-ester, the opacity and cream height also remained unchanged between 24 h and 1 week, which again is consistent with the fact that the corresponding average droplet sizes do not significantly increase over the same time period. However, emulsions with 1 wt % SL-EE, SL-HE, or SL-DE all showed significant surfactant precipitation at both 24 h and 1 week. Given that the SL-esters have low water solubility (<2 mg/mL in deionized H_2O at 25 °C after 1 week),

DOI: 10.1021/acs.langmuir.6b01009

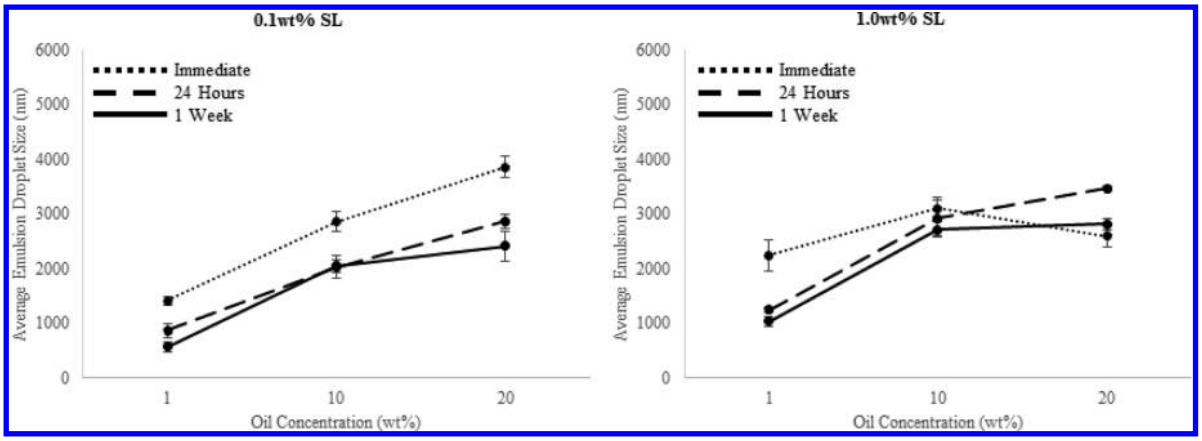

Figure 7. Average emulsion droplet size of LSL + ASL emulsions at 0.1 and 1.0 wt % surfactant concentrations measured immediately after emulsification and after 24 h and 1 week of aging. Mean and standard deviation values are measured from at least three replicates.

the partial precipitation of SL-esters from emulsions is easily rationalized. However, poor water solubility could affect both 0.1 and 1 wt % emulsions. At 1 wt %, SL-ester emulsions of almond oil may be above the saturation concentration of SL-esters at the oil/water interface. In such cases, SL-esters forming micelles in the aqueous phase can precipitate without changing the concentration of SL-esters at the oil/water interface. This scenario is consistent with the overall stability in droplet size over time. That is, if surfactant precipitation is also associated with surfactant desorption from the interface, then the result would be a decrease in the kinetic stability of emulsions that would lead to coalescence and, consequently, increased emulsion size. Presumably, from this analysis, it should be possible to make emulsions with each derivative at the correct concentration such that emulsion droplet sizes are as small as possible without any precipitation.

For comparison to the above studies of SL-esters, the emulsification performance for a 1:1 (w/w) mixture of natural sophorolipids LSL and ASL was analyzed. Images of emulsions that visually describe phase stability and average emulsion droplet sizes are shown in Figures 6 and 7, respectively. Measurements of emulsion droplet sizes were performed at 0.1 and 1.0 wt % LSL + ASL immediately and after aging emulsions for 24 h and 1 week at 25 °C. All LSL + ASL emulsions showed oil separation and precipitation after aging for 24 h and 1 week, with oil separation increasing with increasing oil concentration. LSL precipitation is expected due to its low water solubility (<0.1 mg/mL in deionized H_2O at 25 °C after 1 week). Average emulsion droplet sizes generally decrease with time, indicating oil separation as larger droplets rupture and the oil forms one bulk phase. The emulsion droplet size decrease is not attributed to foaming because it is known that natural SL mixtures exhibit poor foaming.[12] Average emulsion droplet sizes are often smaller than for emulsions formed with the SL-ester, particularly for longer time points, but this is not indicative of increased stability but rather oil separation. These results show that, relative to LSL + ASL 1:1, all of the SL-esters were better able to stabilize almond oil emulsions. This is consistent with the fact that the CAC of LSL + ASL is 4 times higher than that of SL-EE and more than an order of magnitude above that of SL-HE and SL-DE. It is expected that the emulsion stabilization ability of ASL would be far worse than the mixture of LSL + ASL given that the CAC of ASL is greater than 50 mg/mL.

SUMMARY AND CONCLUSIONS

In this work, modified sophorolipids with varying *n*-alkyl ester hydrophobic tail lengths were investigated as surfactants to decrease the interfacial tension and form oil-in-water emulsions of almond oil, a triglyceride rich in oleic and linoleic fatty acids. The length of the SL-ester tail significantly impacts the oil/water IFT and CAC. CAC values were found to correlate with emulsification performance across the SL emulsion formulations studied. This unique connection between CAC and emulsification is expected to facilitate predictions of surfactant performance in future studies with different oil−surfactant systems. Dynamic IFT also pointed to different intersophorolipid and SL-oil interactions as for each SL-ester, particularly when comparing SL-DE to SL-EE and SL-HE.

Modified sophorolipids successfully emulsified almond oil at concentrations 200 times that of the SL-ester used without significant oil separation. However, at higher SL-ester concentrations (1 wt %), precipitation was problematic because of the low solubility of the SL-esters studied herein. It was proposed that lower SL-ester concentrations could be determined that maximize emulsion performance while minimizing SL-ester precipitation. SL-DE has the best emulsification performance on the basis of having the smallest average emulsion droplet sizes of the three SL-esters tested.

Interfacial tension reduction and emulsification were also evaluated for a 1:1 w/w combination of LSL and ASL. The CAC of the mixture was an order of magnitude lower than the SL-esters while the max % IFT reduction and diffusion behavior were similar. The LSL + ASL emulsification showed consistent precipitation and an inability to emulsify low concentrations of almond oil, as is predicted from its relatively high CAC. These results further highlight the positive impact of SL-ester modification on sophorolipid performance.

Future work is planned to expand the range of modified sophorolipids and oil phases studied to better define modified sophorolipid structure−interfacial properties. Through this approach we will learn to tune modified sophorolipid structure to attain high performance for specific challenges. An analysis of the effects of SL-ester structure on interfacial elasticity and rheology as well as the impact of viscosity enhancers on SL-ester emulsions is also planned to expand our current knowledge.

DOI: 10.1021/acs.langmuir.6b01009

■ ASSOCIATED CONTENT

Supporting Information

The Supporting Information is available free of charge on the ACS Publications website at DOI: 10.1021/acs.langmuir.6b01008.

Average emulsion sizes for SL-esters as a function of oil concentrations. ^{1}H and ^{13}C NMR of SL-HE and SL-DE. (PDF)

■ AUTHOR INFORMATION

Corresponding Author

*E-mail: grossr@rpi.edu.

Author Contributions

The manuscript was written through the contributions of all authors. All authors have given approval to the final version of the manuscript.

Notes

The authors declare no competing financial interest.

■ ACKNOWLEDGMENTS

The authors are grateful for funding received from the National Science Foundation Partnerships for International Research and Education (PIRE) Program (award no. 1243313). The authors would also like to thank Dr. Filbert Totsingan and Dr. Dmitri Zagorevski for their help in NMR and LC−MS analysis.

■ REFERENCES

(1) McClements, D. Critical Review of Techniques and Methodologies for Characterization of Emulsion Stability. *Crit. Rev. Food Sci. Nutr.* **2007**, *47*, 611−649.

(2) Marchant, R.; Banat, I. Microbial biosurfactants: challenges and opportunities for future exploitation. *Trends Biotechnol.* **2012**, *30*, 558−565.

(3) Soares, A.; Guieysse, B.; Jefferson, B.; Cartmell, E.; Lester, J. N. Nonylphenol in the environment: A critical review on occurrence, fate, toxicity and treatment in wastewaters. *Environ. Int.* **2008**, *34*, 1033−1049.

(4) Muthusamy, K.; Gopalakrishnan, S.; Ravi, T. K.; Sivachidambaram, P. Biosurfactants: Properties, commercial production, and application. *Curr. Sci.* **2008**, *94*, 736−747.

(5) Marchant, R.; Banat, I. Biosurfactants: a sustainable replacement for chemical surfactants? *Biotechnol. Lett.* **2012**, *34*, 1597−1605.

(6) Gorin, P. A. J.; Spencer, J. F. T.; Tulloch, A. P. Hydroxy fatty acid glycosides of sophorose from torulopsis magnolia. *Can. J. Chem.* **1961**, *39*, 846−855.

(7) Van Bogaert, I.; Saerens, K.; Muynck, C. D.; Develter, D.; Soetaert, U.; Vandamme, E. J. Microbial production of application of sophorolipids. *Appl. Microbiol. Biotechnol.* **2007**, *76*, 23−34.

(8) Felse, P. A.; Shah, V.; Chan, J.; Rao, K. J.; Gross, R. Sophorolipid biosynthesis by Candida bombicola from industrial fatty acid residues. *Enzyme Microb. Technol.* **2007**, *40*, 316−323.

(9) Ratsep, P.; Shah, V. Identification and quantification of sophorolipid analogs using ultra-fast liquid chromatography-mass spectrometry. *J. Microbiol. Methods* **2009**, *78*, 354−356.

(10) de Guzman, D.; Sophorolipids from Mahua Oil. *Green Chem. Blog* 2014 (http://greenchemicalsblog.com/2014/02/14/sophorolipids-from-mahua-oil/) Accessed July 15, 2014.

(11) Mulligan, C. Environmental applications for biosurfactants. *Environ. Pollut.* **2005**, *133*, 183−198.

(12) Hirata, Y.; Ryu, M.; Oda, Y.; Igarashi, K.; Nagatsuka, A.; Furuta, T.; Suguira, M. Novel characteristics of sophorolipids, yeast glycolipid biosurfactants, as biodegradable low-foaming surfactants. *J. Biosci. Bioeng.* **2009**, *108*, 142−146.

(13) Daverey, A.; Pakshirajan, K. Sophorolipids from Candida bombicola using mixed hydrophilic substrates: Production, purification and characterization. *Colloids Surf., B* **2010**, *79*, 246−253.

(14) Ma, X.; Li, H.; Song, X. Surface and biological activity of sophorolipid molecules produced by Wickerhamiella domercqiae var. sophorolipid CGMCC 1576. *J. Colloid Interface Sci.* **2012**, *376*, 165−172.

(15) Maddikeri, G.; Gogate, P.; Pandit, A. Improved synthesis of sophorolipids from waste cooking oil using fed batch approach in the presence of ultrasound. *Chem. Eng. J.* **2015**, *263*, 479−487.

(16) Amine, C.; Dreher, J.; Helgason, J.; Tadros, T. Investigation of emulsifying properties and emulsion stability of plant and milk proteins using interfacial tension and interfacial elasticity. *Food Hydrocolloids* **2014**, *39*, 180−186.

(17) Ampatzidis, C. D.; Varka, E.; Karapantsios, T. D. Interfacial activity of amino acid-based glycerol ether surfactants and their performance in stabilizing O/W cosmetic emulsions. *Colloids Surf., A* **2014**, *460*, 176−183.

(18) Wan, Z.; Wang, L.; Wang, J.; Zhou, Q.; Yuan, Y. Synergistic interfacial properties of soy protein-stevioside mixtures: Relationship to emulsion stability. *Food Hydrocolloids* **2014**, *39*, 127−135.

(19) Ushikubo, F. Y.; Cunha, R. L. Stability mechanisms of liquid water-in-oil emulsions. *Food Hydrocolloids* **2014**, *34*, 145−153.

(20) Zhou, Q. H.; Kosaric, N. Utilization of canola oil and lactose to produce biosurfactant with Candida bombicola. *J. Am. Oil Chem. Soc.* **1995**, *72*, 67−71.

(21) Davila, A. M.; Marchal, R.; Vandecasteele, J. P. Kinetics and balance of fermentation free from product inhibition: sophorose lipid production by Candida bombicola. *Appl. Microbiol. Biotechnol.* **1992**, *38*, 6−11.

(22) Van Bogaert, I.; Fleurackers, S.; Kerrebroeck, S. V.; Develter, D.; Soetaert, W. Production of new to nature sophorolipids by cultivating the yeast Candida bombicola on unconventional hydrophobic substrates. *Biotechnol. Bioeng.* **2011**, *108*, 734−741.

(23) van Bogaert, I. N. A.; Sabirova, J.; Develter, D.; Soetaert, W.; Vandamme, E. J. Knocking out the MFE-2 gene of Candida bombicola leads to improved medium-chain sophorolipid production. *FEMS Yeast Res.* **2009**, *9*, 610−617.

(24) Bisht, K.; Gross, R.; Kaplan, D. Enzyme-mediated regioselective acylations of sophorolipids. *J. Org. Chem.* **1999**, *64*, 780−789.

(25) Azim, A.; Shah, V.; Doncel, G.; Peterson, N.; Gao, W.; Gross, R. Amino Acid Conjugated Sophorolipids: A New Family of Biologically Active Functionalized Glycolipids. *Bioconjugate Chem.* **2006**, *17*, 1523−1529.

(26) Peng, Y.; Totsingan, F.; Meier, M. A. R.; Steinmann, M.; Wurm, F.; Koh, A.; Gross, R. A. Sophorolipids: Expanding structural diversity by ring-opening cross-metathesis. *Eur. J. Lipid Sci. Technol.* **2015**, *117*, 217−228.

(27) Zhang, L.; Somasundaran, P.; Singh, S. K.; Felse, A. P.; Gross, R. A. Synthesis and interfacial properties of sophorolipid derivatives. *Colloids Surf., A* **2004**, *240*, 75−82.

(28) Shin, J. D.; Lee, J.; Kim, Y. B.; Han, I.; Kim, E. Production and characterization of methyl ester sophorolipids with 22-carbon-fatty acids. *Bioresour. Technol.* **2010**, *101*, 3170−3174.

(29) Food and Agriculture Organization of the United Nations; *FAOSTAT−Production−Crops−Almonds, with Shell*; Accessed Nov 6, 2015.

(30) Maestri, D.; Martínez, M.; Bodoira, R.; Rossi, Y.; Oviedo, A.; Pierantozzi, P.; Torres, M. Variability in almond oil chemical traits from traditional cultivars and native genetic resources from Argentina. *Food Chem.* **2015**, *170*, 55−61.

(31) Lorencini, M.; Brohem, C.; Dieamant, G.; Zanchin, N.; Maibach, H. Active ingredients against human epidermal aging. *Ageing Res. Rev.* **2014**, *15*, 100−115.

(32) Draelos, Z. K. Cosmetics: An Overview. *Curr. Probl Dermatol* **1995**, *7* (March/April), 45−64.

(33) Lin, J.; Liu, S.; Hu, C.; Shyu, Y.; Hsu, C.; Yang, D. Effects of roasting temperature and duration on fatty acid composition, phenolic

composition, Maillard reaction degree and antioxidant attribute of almond (Prunus dulcis) kernel. *Food Chem.* **2016**, *190*, 520−528.
(34) Gao, W.; Hagver, R.; Shah, V.; Xie, W.; Gross, R.; Ilker, M.; Bell, C.; Burke, K.; Coughlin, E. Glycolipid Polymer Synthesized from Natural Lactonic Sophorolipids by Ring-Opening Metathesis Polymerization. *Macromolecules* **2007**, *40*, 145−147.
(35) Ward, A. F. H.; Tordai, L. Time-Dependence of Boundary Tensions of Solutions. I. The Role of Diffusion Time-Effects. *J. Chem. Phys.* **1946**, *14*, 453−461.
(36) Campanelli, J.; Wang, X. Dynamic Interfacial Tension of Surfactant Mixtures at Liquid-Liquid Interfaces. *J. Colloid Interface Sci.* **1999**, *213*, 340−351.
(37) Abismaïl, B.; Canselier, J. P.; Wilhelm, A. M.; Delmas, H.; Gourdon, C. Emulsification by ultrasound: drop size distribution and stability. *Ultrason. Sonochem.* **1999**, *6*, 75−83.
(38) Nilsson, F.; Söderstrom, O.; Johansson, I. Physical-Chemical Properties of the N-Octyl β-D-glucoside/Water System. A Phase Diagram, Self-diffusion NMR, and SAXS Study. *Langmuir* **1996**, *12*, 902−908.
(39) Solans, C.; Izquierdo, P.; Nolla, J.; Azemar, N.; Garcia-Celma, M. J. Nano-emulsions. *Curr. Opin. Colloid Interface Sci.* **2005**, *10*, 102−110.
(40) Prasert, W.; Gohtani, S. Effect of temperature on low-energy nanoemulsification and phase behavior in water/polyoxyethylene sorbitan fatty acid ester (Tweens®)/ vegetable oil systems. *J. Food Eng.* **2016**, *180*, 101.
(41) Simjoo, M.; Rezaei, T.; Andrianov, A.; Zitha, P. L. J. Foam stability in the presence of oil: Effect of oil concentration and oil type. *Colloids Surf., A* **2013**, *438*, 148−158.
(42) Sun, C.; Gunasekran, S. Effects of protein concentration and oil-phase volume fraction on the stability and rheology of menhaden oil-in-water emulsions stabilized by whey protein isolate with xanthan gum. *Food Hydrocolloids* **2009**, *23*, 165−174.

DOI: 10.1021/acs.langmuir.6b01909